Palaeogeography, Palaeoclimatology, Palaeoecology 447 (2016) 42–52

Contents lists available at ScienceDirect

Palaeogeography, Palaeoclimatology, Palaeoecology

journal homepage: www.elsevier.com/locate/palaeo

Clay mineralogical and geochemical expressions of the "Late Campanian Event" in the Aquitaine and Paris basins (France): Palaeoenvironmental implications

E. Chenot [a], P. Pellenard [a], M. Martinez [b], J.-F. Deconinck [a], P. Amiotte-Suchet [a], N. Thibault [c], L. Bruneau [a], T. Cocquerez [a], R. Laffont [a], E. Pucéat [a], F. Robaszynski [d,e]

[a] Biogéosciences, UMR 6282, CNRS, University of Bourgogne Franche-Comté, 6 boulevard Gabriel, Dijon F-21000, France
[b] MARUM, Center for Marine Environmental Sciences, Universität Bremen, Leobener Str., Bremen D-28359, Germany
[c] IGN, University of Copenhagen, Øster Voldgade 10, Copenhagen DK-1350, Denmark
[d] Faculté Polytechnique, Université de Mons, 9 rue de Houdain, Mons 7000, Belgium
[e] 57 rue Desmortiers, Saintes 17100, France

ARTICLE INFO

Article history:
Received 2 September 2015
Received in revised form 21 January 2016
Accepted 22 January 2016
Available online 29 January 2016

Keywords:
Campanian
Late Campanian Event
Clay minerals
Carbon isotope stratigraphy
Cyclostratigraphy

ABSTRACT

Campanian sediments from two French sedimentary basins were studied, using clay mineralogy and stable isotope ($\delta^{13}C$ and $\delta^{18}O$) geochemistry, in order to investigate the Late Campanian Event. The clay fraction of the Campanian sediments from the Tercis-les-Bains section (Aquitaine Basin) and from the Poigny borehole (Paris Basin) is mainly composed of smectite. This background sedimentation was, however, interrupted during the Upper Campanian in the two basins by a substantial increase in detrital inputs, including illite, kaolinite, and chlorite at Tercis-les-Bains, and illite at Poigny. This detrital event, resulting from the enhanced erosion of nearby continental areas triggered by increasing runoff, has also been recognized in the Tethys and South Atlantic oceans. It coincided with a global negative carbon isotope excursion, the Late Campanian Event (LCE). Carbon isotope stratigraphy was used to correlate the two basins with previously studied sections from distant areas. Spectral analysis of the bulk $\delta^{13}C$ from Tercis-les-Bains suggests a duration of *ca.* 400 kyr for a pre-LCE negative excursion and *ca.* 800–900 kyr for the LCE *sensu stricto*. The detrital event, as characterized by clay mineralogy, spans the interval that comprises the pre-LCE and the LCE, with a duration of 1.3 Myr. Intensification of continental erosion during the LCE may have resulted either from the Late Campanian *polyplocum* regression and/or from a regional tectonic pulse that triggered the emersion of previous submerged shelf areas and the increase of silicate erosion. As the LCE seems to be recorded at a large geographic scale, it is proposed here that enhanced chemical weathering and an associated decrease in atmospheric pCO_2 levels could have contributed to the long-term Late Cretaceous cooling trend.

1. Introduction

The Cretaceous is a "greenhouse" period with maximum sea-surface temperatures recorded around the Cenomanian to Turonian interval (Jenkyns et al., 1994; Clarke and Jenkyns, 1999; Pucéat et al., 2005; Friedrich et al., 2012). Following this climatic optimum, isotopic data highlight a long-term cooling during the remainder of the Late Cretaceous (Huber et al., 1995; Clarke and Jenkyns, 1999; Friedrich et al., 2012; Linnert et al., 2014). This cooling trend accelerated during the beginning of the Campanian (Friedrich et al., 2012, Linnert et al., 2014), but its mechanisms and dynamics are not yet well understood. The Campanian is also characterized by significant fluctuations of the sea level (Haq et al., 1987; Barrera et al., 1997; Jarvis et al., 2002), a major shift in the $\delta^{15}N$ of marine organic matter (Algeo et al., 2014), clay mineralogical changes, and the occurrence of positive and negative carbon isotope events: the Santonian–Campanian Boundary Event (SCBE) (Jarvis et al., 2002, 2006), the Mid Campanian Event (MCE) (Jarvis et al., 2002, 2006; Thibault et al., 2012a), the *conica* Event (Perdiou et al., 2015), the Late Campanian Event (LCE) (Jarvis et al., 2002, 2006; Voigt et al., 2012; Thibault et al., 2012a, b), the Epsilon Event (EE) (also called C1- Event) (Thibault et al., 2012a, 2015), and the Campanian–Maastrichtian Boundary Event (CMBE) (Barrera, 1994; Barrera and Savin, 1999; Friedrich et al., 2009; Jung et al., 2012; Voigt et al., 2012; Thibault et al., 2012a, 2015). Mineralogical changes expressed by detrital inputs of kaolinite and illite have been observed in many sedimentary basins, including the South Atlantic Ocean (Chamley et al., 1984), the Umbria-Marche Basin (Deconinck, 1992), the Saharan Platform (Li et al., 2000), and in the Paris Basin (Deconinck et al., 2005). As these mineralogical changes are stratigraphically poorly constrained, they cannot be associated with isotopic events. The objective here is to better understand the Campanian palaeoclimatic cooling by an integrated study of clay mineralogy and

http://dx.doi.org/10.1016/j.palaeo.2016.01.040

isotope geochemistry ($\delta^{13}C$ and $\delta^{18}O$). In addition, a cyclostratigraphic study was conducted in order to estimate the duration of the clay mineral change during the LCE.

We focus on two French sedimentary basins, the Aquitaine and the Paris basins. Isotopic data from the Tercis-les-Bains section (Aquitaine Basin) published by Voigt et al. (2012) are compared with new clay mineralogical data, while clay mineralogical data from the Poigny borehole (Paris Basin) published by Deconinck et al. (2005) are compared with new isotopic data. The whole data set is used to better constrain the timing of clay mineralogical changes and isotopic events that occurred in both basins.

2. Palaeogeography and geological settings

During the Campanian, the Atlantic Ocean was widening, while the Tethys Ocean was in the process of closing due to the counterclockwise motion of Africa (Smith, 1971; Dewey et al., 1973; Blakey, 2008). This period corresponded to the development of epicontinental seas in the Tethyan realm. Western Europe was an archipelago, whose islands corresponded to emergent Hercynian massifs (*e.g.,* Armorican, Central, and Rhenian Massifs) separated by epicontinental seas (Fig. 1). These emergent lands locally contributed to terrigenous sedimentation, although most Campanian sediments in the studied basins are composed of chalk and bioclastic limestone beds.

2.1. The Tercis-les-Bains section

The studied section is located in an abandoned quarry near Tercis-les-Bains (north-west of Dax) and belongs to the Aquitaine Basin (south-west France, Fig. 1). This basin was in an intermediate position between the North Atlantic and the Tethyan oceans (Fig. 1). The Tercis-les-Bains quarry, opened on the side of a diapir, shows vertically oriented Late Campanian to Maastrichtian beds (Bilotte et al., 2001; Odin, 2001). The 116-m-thick Campanian succession is composed of bioclastic limestone beds with common glauconitic horizons, flint nodules, and occasional marly levels (Fig. 2). The relatively homogeneous facies, microfacies, and faunal associations reflect deposition on the outer shelf in lower offshore environments (Berthou et al., 2001). The section is defined as the Global boundary Stratotype Section Point (GSSP) of the base Maastrichtian Stage (Odin, 2001), ensuring a well-defined magnetostratigraphic and biostratigraphic framework for the middle and upper part of the Campanian (Fig. 3).

2.2. The Poigny borehole

A thick succession of chalk (about 700 m), deposited from the Cenomanian to the Campanian, was drilled at Poigny, south-east of Paris (Craie 700 project, Mégnien and Hanot, 2000; Fig. 1). The Paris Basin was surrounded by the London-Brabant Massif to the north, by the Massif Central to the south and by the Armorican Massif to the west (Fig. 1). During the Late Cretaceous, the Paris Basin was an epicontinental sea where chalk accumulated. It was connected with the Tethys to the south-east, with the Boreal Ocean to the north and with the North Atlantic to the west. The lithological description of the borehole includes marker beds and biostratigraphic data based on benthic foraminifera, dinoflagellates, ostracods, nannofossils, and bivalves (Fig. 4), which allowed a detailed stratigraphic framework of the ~250-m-thick Campanian succession to be established (Robaszynski et al., 2005). Unfortunately, planktonic foraminifera cannot be studied in the Campanian succession of the Poigny borehole due to their poor preservation,

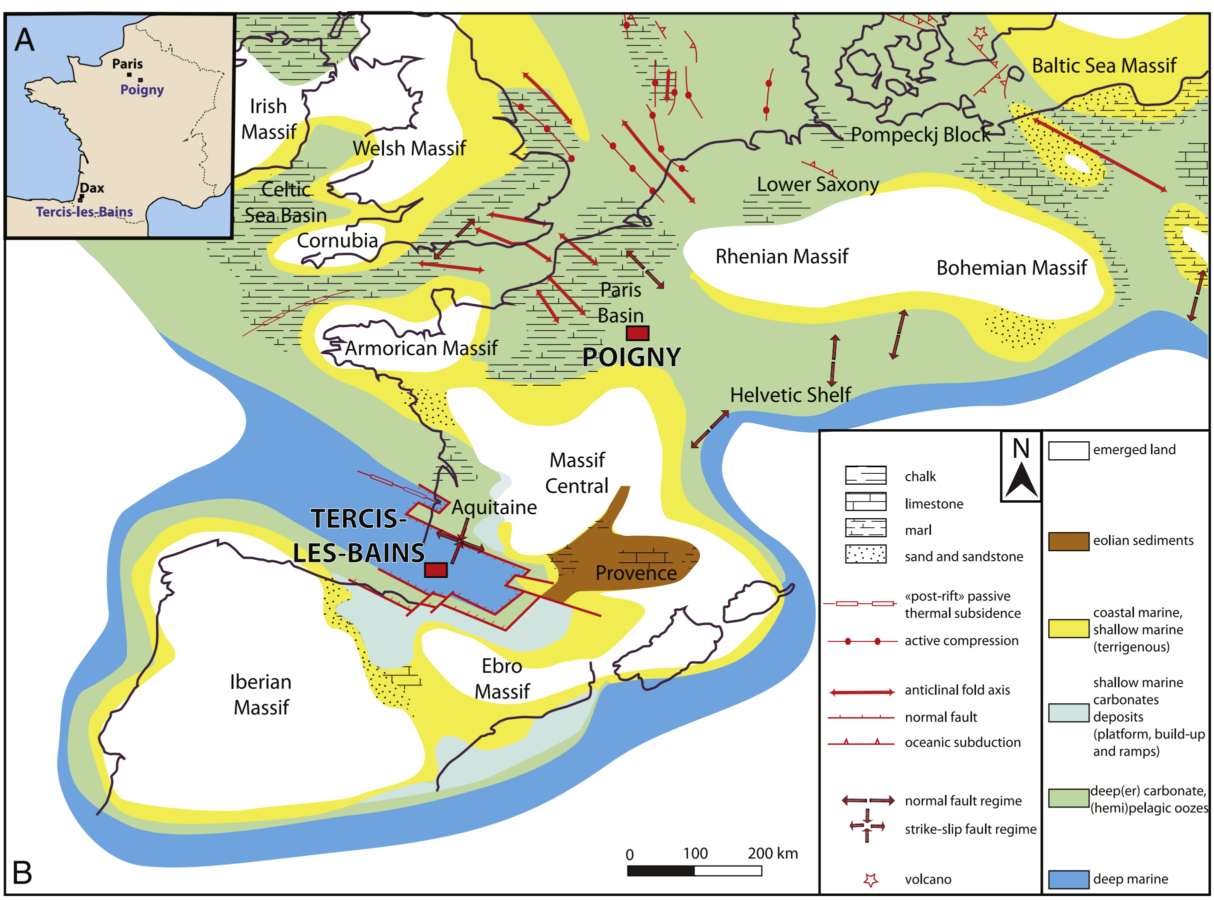

Fig. 1. Studied sites located on (A) a geographic map and (B) on a palaeogeographic map of the Western Peri–Tethyan Realm during the Early Campanian (modified after Philip and Floquet, 2000).

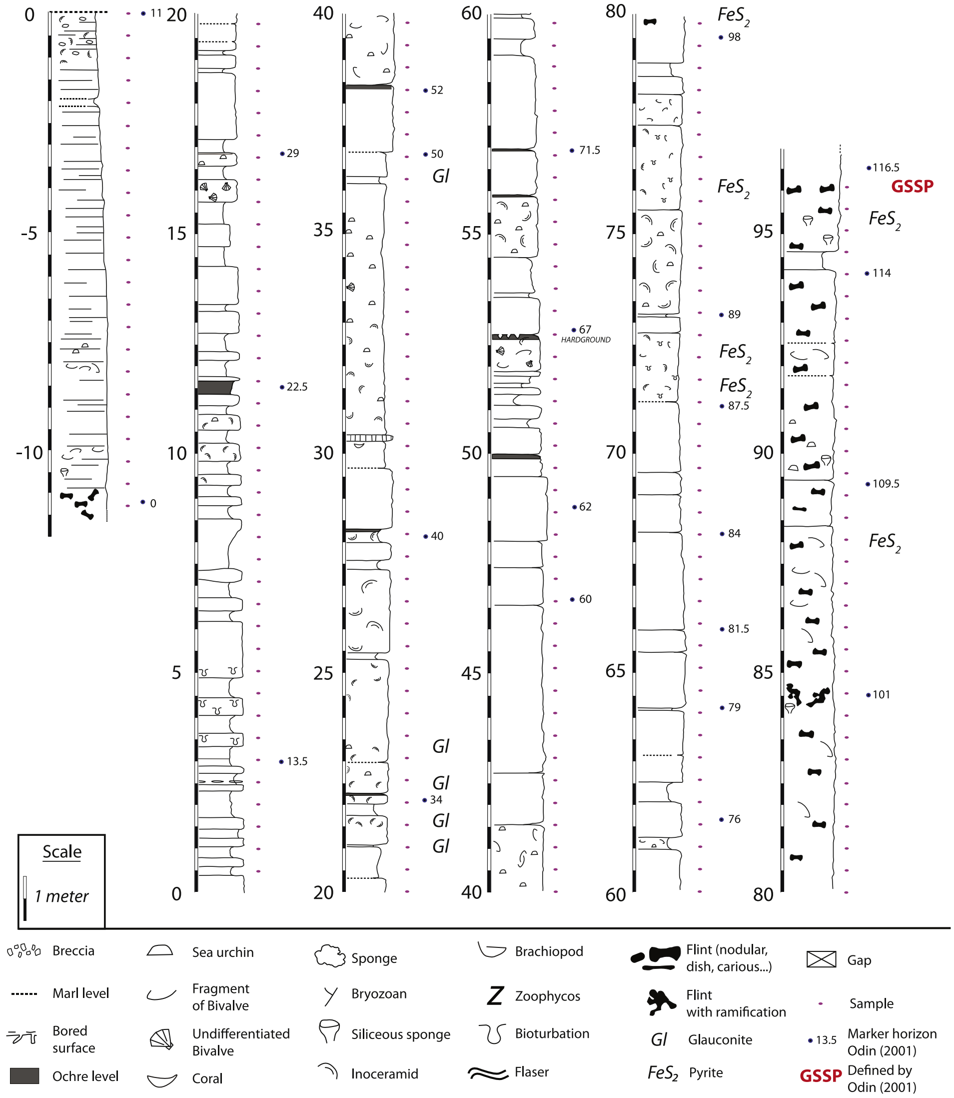

Fig. 2. Detailed lithology and sample location (purple points) for the Campanian of Tercis-les-Bains. GSSP mark at 96 m corresponds to the base of the Maastrichtian Stage, defined by Odin (2001).

but some markers are present in the Cenomanian–Turonian interval. Through bio- and lithostratigraphic arguments, the Santonian–Campanian boundary has been identified between 285 and 290 m (Robaszynski et al., 2005). A major erosion event during the early Tertiary was responsible for the absence of uppermost Campanian and Maastrichtian chalk deposits (Mettraux et al., 1999; Guillocheau et al., 2000; Lasseur, 2007).

3. Materials and methods

3.1. Clay mineralogy

In the Tercis-les-Bains quarry, bulk-rock samples were collected at a sample interval of 50 cm (Fig. 2). Mineralogical analyses were performed at the Biogéosciences Laboratory, University of Bourgogne Franche-Comté, Dijon, France. Clay mineral assemblages of 212 samples devoid of flint were identified by X-ray diffraction (XRD) on oriented mounts of non-calcareous clay-sized particles (<2 μm). The procedure described by Moore and Reynolds (1997) was used to prepare the samples. Diffractograms were obtained using a Bruker D4 Endeavor diffractometer with CuK_{α} radiations with LynxEye detector and Ni filter, under 40-kV voltage and 25-mA intensity. Three preparations were analyzed, the first after air-drying, the second after ethylene-glycol solvation, and the third after heating at 490 °C for 2 h. The goniometer was scanned from 2.5° to 28.5° for each run. Clay minerals were identified by the position of their main diffraction peaks on the three XRD runs, while semi-quantitative estimates were produced in relation to their area (Moore and Reynolds, 1997). Areas were determined on diffractograms of glycolated runs with MacDiff 4.2.5. Software (Petschick, 2000). Beyond the evaluation of the absolute proportions of the clay minerals, the aim was to identify their relative fluctuations along the section. Peaks close to 14 Å in air-dried conditions and 17 Å after ethylene-glycol solvation are random R0 type illite/smectite mixed-layers (60–80% of smectite sheets on average according to Inoue et al., 1989 and Moore and Reynolds, 1997). In the result and discussion sections, the term smectite, as classically employed by sedimentologists, is used to refer to these minerals (Chamley et al., 1990; Deconinck et al., 2005, Pellenard and Deconinck, 2006). The smectite/illite ratio (S/I) corresponds to the ratio between the 17-Å peak area and the 10-Å peak area (defined as illite), after ethylene-glycol solvation.

3.2. Stable isotope geochemistry

Wherever possible, samples were recovered every meter from the Poigny borehole for geochemical analyses. Isotopic analyses ($\delta^{13}C$ and

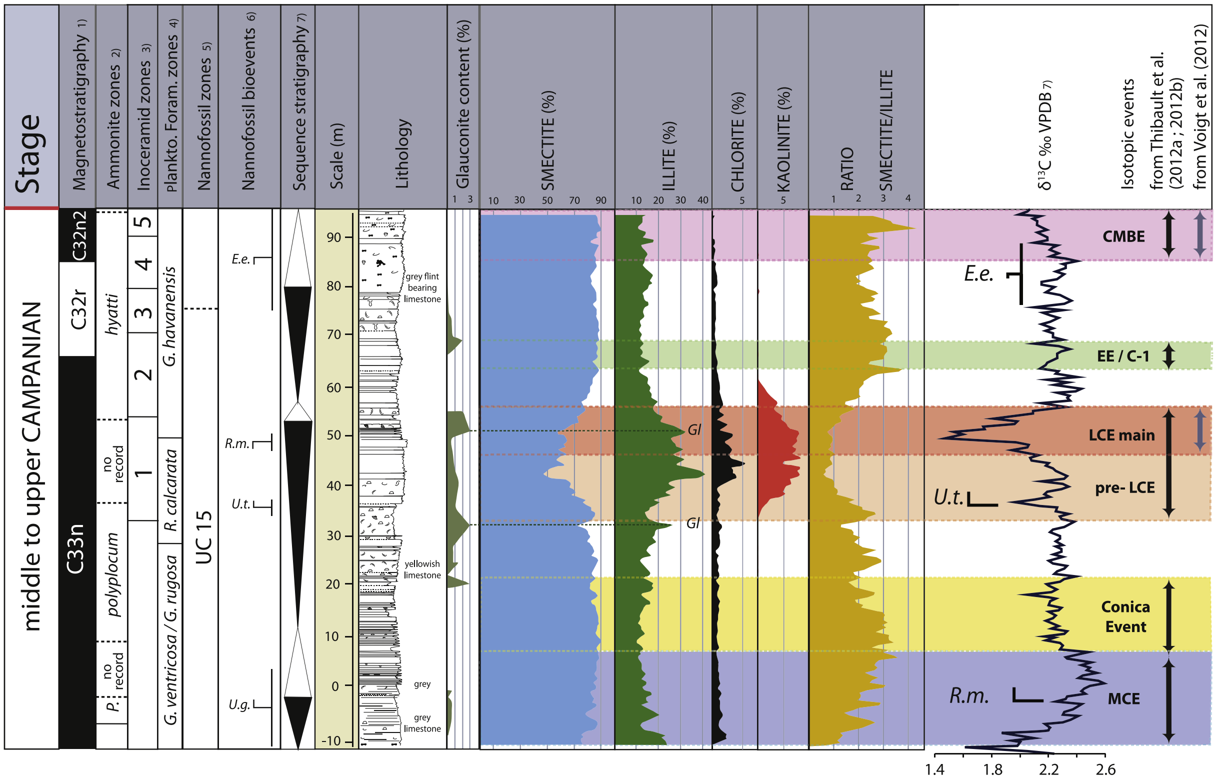

Fig. 3. Clay mineralogy of the Campanian at Tercis-les-Bains compared with the carbon isotope stratigraphy from Voigt et al. (2012), with the two different isotopic interpretations of Voigt et al. (2012) and of Thibault et al. (2012a, 2001b). References: (1) Odin and Lamaurelle (2001), Lewy and Odin (2001); (2) Odin et al. (2001b); (3) Walaszczyk et al. (2002); (4) Odin et al. (2001a); (5) Melinte and Odin (2001); (6) Gardin et al. (2001); (7) Voigt et al. (2012); Odin (2001). Abbreviations: *E.e.* = *Eiffellithus eximius*; *G.ventricosa/G.rugosa* = *Globotruncana ventricosa/Globotruncana rugosa*; *P.* = *Pseudoxybeloceras* sp.; *R.m.* = *Rucinolithus magnus*; *U.g.* = *Uniplanarius gothicus*; *U.t.* = *Uniplanarius trifidus; Gl* = glauconite.

$\delta^{18}O$) were performed on 243 samples of bulk sediment along the whole section from the Santonian–Campanian boundary to the Late Campanian. Unfortunately, due to the Tertiary erosion, the uppermost part of the Campanian is missing and the yellowish chalk succession observed in the topmost part of the core probably indicates the circulation of meteoric fluids (Fig. 4). Isotope analyses were performed at the

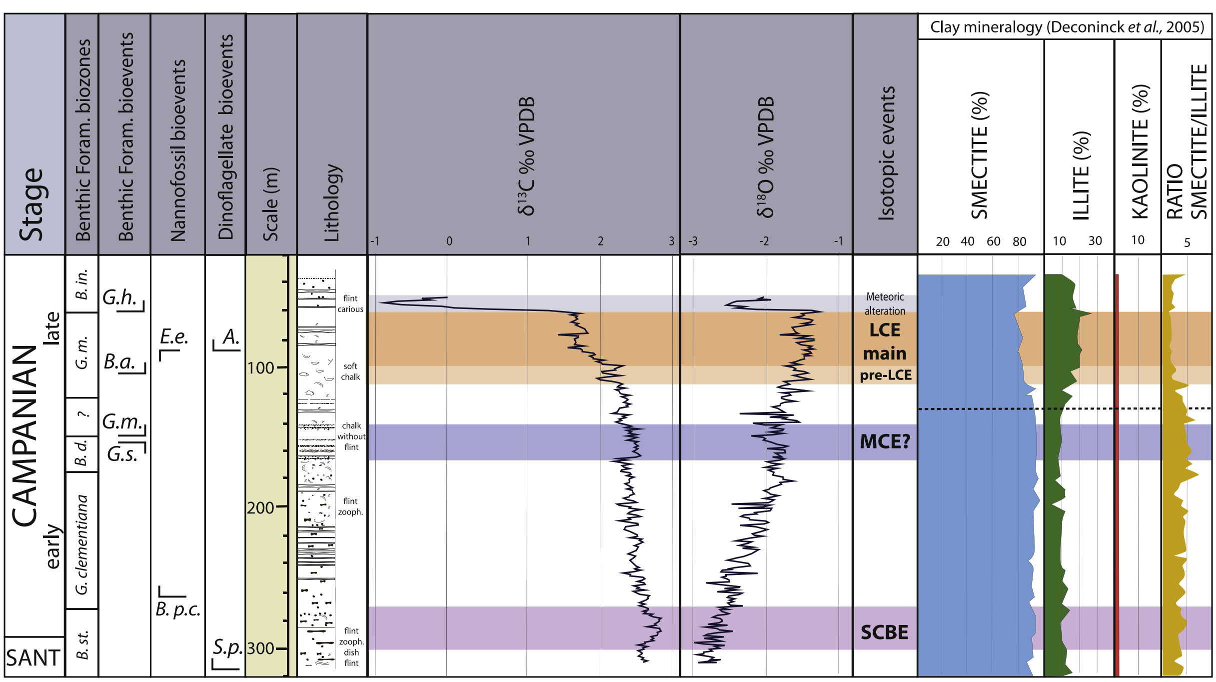

Fig. 4. Isotope data of the Poigny borehole compared to the mineralogical data from Deconinck et al. (2005). The dashed line corresponds to the mineralogical change identified by Deconinck et al. (2005). The figure caption used to describe the lithology is the same as Fig. 2. Abbreviations: *A.* = *Areoligera; B.a.* = *Bolivinoides australis; B.d.* = *Bolivinoides decoratus; B.in.* = *Bolivina incrassata; B.p.c.* = *Broinsonia parca constricta; B.st.* = *Bolivinoides strigillatus; E.e.* = *Eiffellithus eximius; G.h.* = *Globotruncanella havanensis; G.m.* = *Gavelinella monterelensis; G.s.* = *Gavelinella stelligera; S.p.* = *Senoniasphaera protrusa;* LCE = late Campanian event; MCE = mid Campanian event; SCBE = Santonian–Campanian Boundary Event.

Biogéosciences Laboratory, University of Bourgogne Franche-Comté, Dijon, France. Calcite powders from samples devoid of macrofossils were reacted with 100% phosphoric acid at 90 °C, using a Multiprep on-line carbonate preparation line connected to an Isoprime mass spectrometer. All isotopic values are reported in the standard δ-notation in per mil relative to V-PDB (Vienna Pee Dee Belemnite) by assigning a δ^{13}C value of +1.95‰ and a δ^{18}O value of −2.20‰ to NBS19. Reproducibility was checked by replicate analysis of laboratory standards and is ±0.08‰ (2σ) for oxygen isotopes and ±0.04‰ (2σ) for carbon isotopes.

3.3. Cyclostratigraphy

Spectral analyses were conducted on isotopic data (δ^{13}C) to detect orbital cycles and to estimate the duration of the LCE in the Tercis-les-Bains section.

The δ^{13}C series shows a marked negative shift in δ^{13}C values (1‰) previously identified as the LCE (Voigt et al., 2012). This shift and the long-term trends were removed by applying a best-fit piecewise linear regression; the series was then standardized (mean = 0; standard deviation = 1). The spectrum of the AR(1) pre-whitened series was calculated using the multi-taper method, applying three 2π tapers (Thomson, 1982, 1990). The low-spec method was then used to calculate the spectrum background of the pre-whitened series and the confidence levels (Meyers, 2012, 2014). A time-frequency weighted fast Fourier transform (T-F WFFT) applying 30-m-width windows was performed to follow the evolution of the main periods throughout the δ^{13}C series (Martinez et al., 2013, 2015). The method consists in dividing the series into a series of intervals of 30-m width separated from each other by 0.5 m. In each interval, the local trend in the average is removed by subtracting a linear regression from each interval of the series. Each of the intervals is then weighted using one Slepian sequence and a Fast Fourier Transform is calculated on each of the weighted signals. The result is a 3-dimensional spectrum, called spectrogram, showing in blue the spectrum background and in red the highest powers. A Taner band-pass filter was then applied to isolate the cycles of interest (Taner, 2003).

4. Results

4.1. Tercis-les-Bains

At Tercis-les-Bains, the clay mineral assemblages are predominantly (more than 80%) composed of random illite/smectite mixed-layers (IS R0), hereafter referred to as smectite (Fig. 3). Other clay minerals, including illite (generally less than 20%) and traces of chlorite (less than 5%), occur in most samples (Fig. 3). Kaolinite is absent except within the interval from 33 to 62.5 m. In this interval, the kaolinite content significantly increases up to 8% together with more abundant illite and chlorite. This major change in the clay mineral assemblages matches preliminary data (Odin, 2001) and is the most striking feature of the section. The kaolinite-bearing interval starts concomitantly to the first occurrence (FO) of the calcareous nannofossil *Uniplanarius trifidus*, straddles the *Radotruncana calcarata* zone and *Globotruncanella havanensis* zone, and ends above the last occurrence (LO) of the calcareous nannofossil *Rucinolithus magnus*. Interestingly, the increase in kaolinite, illite, and chlorite contents coincides with the negative δ^{13}C excursion that defines the LCE (Fig. 3).

The multi-taper analysis (Fig. 5C) indicates two significant peaks at 8.6 m (>99% confidence level) and at 1.2 m (>95% confidence level). However, the peak at 1.2 m is close to the Nyquist frequency, which is at 1.25 cycles/m (*i.e.*, 0.8 m), and is not interpreted here. Results of the T-F WFFT suggest that the peak identified at 8.6 m actually corresponds to a high-power frequency band whose average period is observed with a period of 7.4 m from the base of the series to level ~ 120 m and evolves to a period of 4.9 m from level ~ 120 m to the top of the series (Fig. 5D). Small peaks around this 4.9-m period appear on the multi-taper method (MTM) power spectrum but they are poorly significant, their power being probably hidden by that of the overall 8.6-m band, which appears more consistent from the base of the time-series up to *ca.* 120 m (Fig. 5). After filtering the band of ~8–5 m using a Taner band-pass filter, a total of 23 to 24 repetitions of this cycle are observed throughout the series (Fig. 5B). In agreement with the spectrogram, this filtered signal displays its maximum of amplitude from 40 to 60 m in depth, in the interval containing the LCE (Fig. 5B and D).

4.2. Poigny

In the Poigny borehole, bulk-rock δ^{13}C isotopic values show an overall decreasing trend from values of about 2.7‰ at the base of the series to values of about 1.7‰ at 59 m (Fig. 4), with an acceleration of the decreasing trend from 126 m upward, *i.e.*, from the FO of *Gavelinella monterelensis* to below the FO of *G. havanensis*. This trend is interrupted by two moderate positive isotopic excursions. The first excursion of 0.3‰ starts at a depth of 304 m above the FO of the foraminifera *Gavelinella cristata* and ends at a depth of 266 m below the FO of the nannofossil *Broinsonia parca constricta*. The second excursion of 0.3‰ occurs from 164.25 m to 138.25 m and coincides with the LO of *Gavelinella stelligera* and the FO of *G. monterelensis*. The last part of the borehole (from 59 to 50 m) is characterized by a large negative excursion of over 2.5‰, with values reaching −1‰.

Bulk-rock δ^{18}O values display an increasing trend from −2.7‰ at the base of the section to values of about −1.5‰ at top of the section (Fig. 4). The top of the section is characterized by a negative excursion of about 1‰ in δ^{18}O values that coincides with the lowest recorded δ^{13}C values.

5. Discussion

5.1. Influence of diagenesis

Before interpreting the clay mineral successions in terms of palaeoenvironments, it is necessary to evaluate the influence of diagenesis. In both studied sedimentary successions, the occurrence of smectite indicates negligible influence of burial diagenesis, as these minerals are very sensitive to temperature increase, with illitization starting at about 60 °C (Środoń, 2009). According to the geological history of the Paris Basin (Brunet and Le Pichon, 1982), a 500-m-burial depth was estimated at Poigny, not deep enough to trigger incipient illitization. In this borehole, clay minerals are thus mainly considered as detrital (Deconinck et al., 2005; Fig. 4). Similarly, the occurrence of smectite at Tercis-les-Bains indicates a minor influence of burial diagenesis (Fig. 3). The presence of glauconitic granules, generally less than 1% (Odin and Amorosi, 2001; Fig. 3), implies that illite identified by XRD (10-Å peak) consists of a mixture of a major detrital component with minor authigenic glauconitic minerals formed during early diagenesis. The amounts of glauconite reaching 1–3% only occur in three thin well-identified horizons indicative of lower sedimentation rates (Fig. 3).

In the Poigny borehole, the upper part of the chalk is yellowish, in marked contrast to the remainder of the core. This yellowish chalk has a low Mg content and has therefore been interpreted as alteration caused by meteoric fluids during the post-Cretaceous emersion (Le Callonnec et al., 2000). The isotopic results for the upper part of the Poigny core (59–50 m; Fig. 5) are characterized by a negative excursion of about 1‰ in δ^{18}O values that coincides with the lowest δ^{13}C values. A crossplot of carbon- and oxygen-isotope data from the Poigny borehole (Fig. 6) highlights the difference in isotopic composition between the samples from the yellowish chalk (59 to 50 m; red dots) and those from the remainder of the section (309 to 59 m; blue dots). The data were therefore treated as two separate subsets, and a Spearman's coefficient was computed for each of these subsets to test the existence of any correlation within the data. This coefficient was

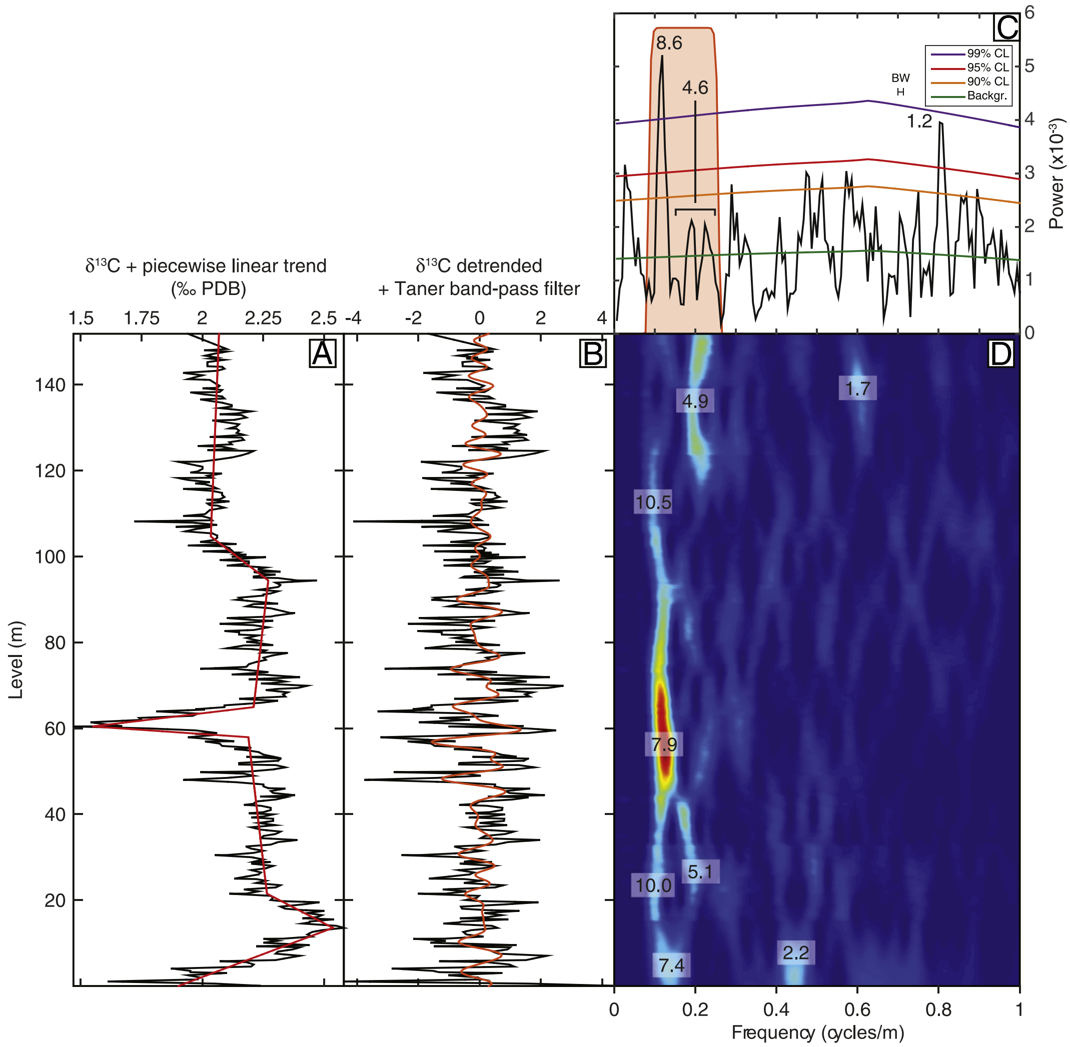

Fig. 5. Spectral analyses of the $\delta^{13}C$ series. (A) Raw $\delta^{13}C$ series (in black) with best-fit piecewise linear regression (in red). (B) Filtering of the $\delta^{13}C$ series. *In black*: standardized $\delta^{13}C$; *in orange*: band-pass filter of the 8–5-m band (lower frequency cut: 9.155×10^{-2} cycles/m; upper frequency cut: 2.625×10^{-1} cycles/m; roll-off rate: 10^{12}). (C) 2π multi-taper spectrum of the standardized $\delta^{13}C$ series. Confidence levels are calculated using the low-spec method (Meyers, 2012) with the script available in the 'astrochron' R package (Meyers, 2014). (D) Time-frequency weighted fast Fourier transform performed with 30-m-width windows. Red colors indicate the highest values of power (*i.e.*, the main cycles) and blue indicate the lowest values of power. Main-power periods are labeled in meters.

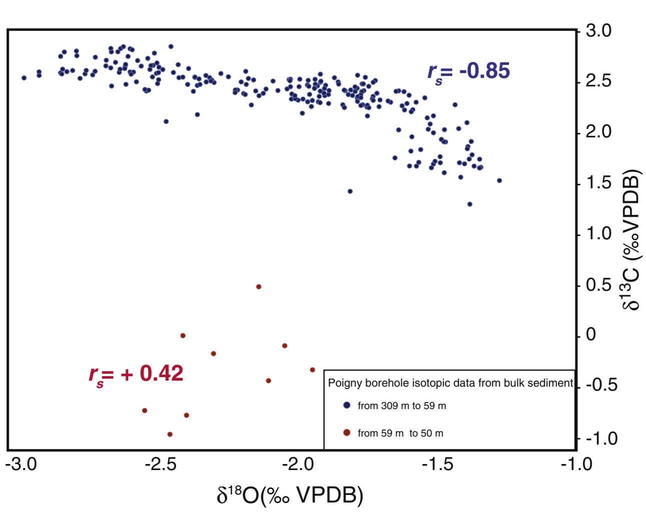

Fig. 6. Cross plot of carbon- and oxygen- isotopes values of Poigny borehole. Data are from bulk sediment samples. r_s corresponds to the Spearman's coefficient correlation values.

chosen because of the non-linear nature of the relationship between the two variables, $\delta^{13}C$ and $\delta^{18}O$. Values of 1 indicate perfect correlation, values of −1 indicate perfect anti-correlation, while 0 indicates absence of correlation. From 309 to 59 m, $\delta^{13}C$ and $\delta^{18}O$ values are negatively correlated, with a Spearman coefficient of $r_s = -0.85$, whereas $\delta^{13}C$ and $\delta^{18}O$ values are positively correlated from 59 to 50 m, with a Spearman coefficient of $r_s = +0.42$. In marine carbonates, the positive correlation of $\delta^{13}C$ and $\delta^{18}O$ values can be explained by several mechanisms, such as kinetic effects recorded within the shells of some organisms (McConnaughey, 1989a, 1989b; McConnaughey et al., 1997; Wenzel et al., 2000; Auclair et al., 2003; Gillikin et al., 2006), or co-variations of seawater temperature and local primary productivity, associated with remineralization of organic matter at depth (*e.g.*, Kirby et al., 1998). However, positive correlation can also be observed as the result of diagenesis, when it is extensive enough to affect carbon isotope composition, which is usually less prone to diagenetic alteration. The influence of meteoric fluids during telogenesis is one form of diagenesis known to produce yellowish alteration of chalk (Le Callonnec et al., 2000). The telogenesis hypothesis can be justified for the first data subset (59–50 m) by two factors: (1) the specific aspect of the chalk and (2) the positive correlation between $\delta^{13}C$ and $\delta^{18}O$ values. In contrast, no positive correlation was observed for the second data subset (309–59 m), which suggests a negligible diagenetic effect on $\delta^{13}C$ values for most of the core.

5.2. Identifying C-isotopic events and correlation with other sections in Europe

At Poigny, the Santonian–Campanian boundary is located between 290 m and 285 m, based on benthic foraminiferal bioevents (Robazsynski et al., 2005). This is consistent with the 0.3‰ $\delta^{13}C$ positive excursion recorded in this interval, which is therefore attributed to the SCBE (Fig. 4).

A slight increase of $\delta^{13}C$ occurring between 164.25 and 138.25 m is tentatively attributed to the MCE (Fig. 4), and the clear trend toward lower values of $\delta^{13}C$, from 112 to 59 m, corresponds to the lower part of the LCE. Several biostratigraphic criteria preclude the attribution of this negative excursion to the CMBE because (1) among benthic foraminifera considered to be good markers of the Campanian–Maastrichtian boundary, *Neoflabellina reticulata* is not present, and (2) the LO of *Eiffellithus eximius* occurs at the base of the Late Campanian *R. calcarata* zone in the Kalaat Senan section (Tunisia; Robaszynski et al., 2000), within the uppermost part of Chron C33n and just below the base of the *R. calcarata* zone in the Bottaccione section (Italy, Gardin et al., 2012), and in the Late Campanian *polyplocum* zone in the Lägerdorf–Kronsmoor section (Voigt and Schönfeld, 2010). This nannofossil biostratigraphic marker is also recorded in the early Late Campanian in Norfolk (England, Jarvis et al., 2002), Tercis-les-Bains (Gardin et al., 2001) and in the ODP Hole 762C (Thibault et al., 2012b).

Carbon isotopes are widely used to correlate sections around the globe (*e.g.*, Scholle and Arthur, 1980) and may be a useful tool if diagenetic influences on $\delta^{13}C$ are carefully considered (Wendler, 2013). A large number of carbon isotope events have been widely recognized from the Coniacian to the Maastrichtian and defined in the $\delta^{13}C$ reference curve of the English chalk (Jarvis et al., 2002). In the GSSP of Tercis-les-Bains, Thibault et al. (2012a) have notably recognized the three-step negative shifts of the $\delta^{13}C$ of the CMBE (CMBa, CMBb, CMBc). In the Late Campanian, the EE (or C1 Event; Thibault et al., 2012a, 2015) defined as a slight negative excursion of the carbon–isotope curve is recorded in the Stevns-1 borehole (Danish Basin; Thibault et al., 2012a), in the ODP 762C Hole (Indian Ocean; Thibault et al., 2012b), and in the chalk of Lägerdorf–Kronsmoor section (Boreal Ocean, Thibault et al., 2012b; Figs. 3 and 7).

In the high-resolution carbon–isotope data of Tercis-les-Bains, the LCE appears as a major excursion of −1‰ between 53 and 70 m but is immediately preceded by a sharp −0.4‰ excursion between 45 and 53 m, that we name here pre-LCE following Perdiou et al. (2015; Fig. 3). These authors identified two significant stepwise negative shifts prior to the LCE in the North Sea that they defined as pre-LCE, correlated to Lägerdorf–Kronsmoor and interpreted as an amplification of the pacing of the carbon cycle by the 405-kyr eccentricity preceding the main LCE (Perdiou et al., 2015). We propose here to position the pre-LCE and the LCE excursions based on the most positive value recorded

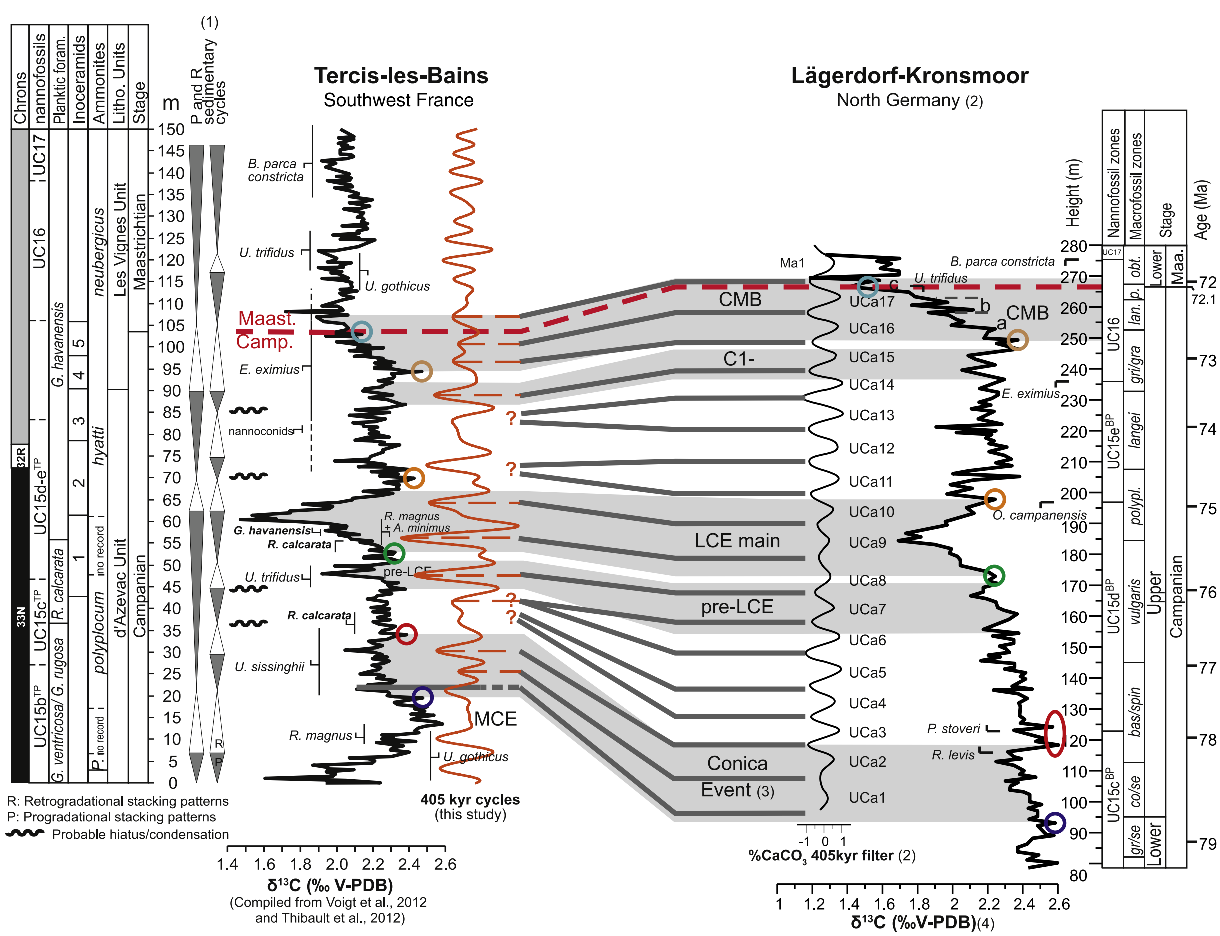

Fig. 7. Proposed correlation of carbon isotopes curves and 405-kyr cycles between the Tercis-les-Bains section and Lägerdorf–Kronsmoor section. This correlation is supported by the tie-points of isotopic curves highlighted by the colored circles. Comparison of the 405-kyr cycles suggests a number of hiatuses at Tercis-les-Bains, which is line with the sequence stratigraphic interpretation; 72.1 Ma indicates the absolute age of the Campanian–Maastrichtian boundary. (1) Voigt et al. (2012), (2) Voigt and Schönfeld (2010), (3) Conica Event as defined by Perdiou et al., 2015, (4) Voigt et al., 2010. Abbreviations: *bas./spin.* = *basiplana/spiniger*; *con./sen.* = *conica/senonencis*; *gri./gra.* = *grimmensis/granulosis*; *G.v./G.r.* = *Globotruncana ventricosa/Globotruncana rugosa*; *P* = *Pseudoxybeloceras* sp.; *R.c.* = *Radotruncana calcarata*; *G. havanensis* = *Globotruncana havanensis*.

at the base and at the top of each negative excursion. Correlation with Lägerdorf–Kronsmoor suggests that a number of pre-LCE excursions may be also identified there between 145 and 170 m (Fig. 7). Correlation of 405-kyr cycles and carbon isotope variations between the Lägerdorf–Kronsmoor section and the North Sea core Adda-3, where Perdiou et al. (2015) define their pre-LCE excursions, suggests that the pre-LCE interval at Lägerdorf–Kronsmoor includes the two small stepwise 0.2 to 0.3‰ negative shifts at *ca.* 155 and 165 m (Fig. 7). Therefore, the sole −0.4‰ excursion recorded in Tercis-les-Bains that precedes the LCE is correlated here to the whole interval that includes these two negative shifts at Lägerdorf–Kronsmoor (Fig. 7). At Poigny, a rather similar record is observed with the occurrence of pre-LCE stepwise negative excursions between 112 and 59 m, immediately preceding the lower part of the LCE marked by a transient progressive 0.8‰ negative excursion from 100 to 85 m (Fig. 4). The positive shift that constitutes the upper half of the LCE is hindered at Poigny by the level of intense alteration that shifts the $\delta^{13}C$ and the $\delta^{18}O$ toward very negative values (highlighted in gray in Fig. 4).

In the lowermost part of the Upper Campanian, a long-lasting excursion of *ca.* −0.3‰ immediately follows the MCE at Tercis-les-Bains between 35 m and 20 m. This excursion is characterized by steady $\delta^{13}C$ values around 2.25‰, a sharp negative shift at the base following the MCE, and a sharp positive shift at the top, coinciding with the FO of *R. calcarata*. This excursion correlates with a similar trend at Lägerdorf–Kronsmoor observed from 93 to 120 m within UC15c^{BP} (Figs. 3 and 7). This excursion has also been identified in the Adda-3 borehole (North Sea) and recently defined as the *conica* Event by Perdiou et al. (2015).

5.3. Duration of the LCE

In the Geological Time Scale 2012 (Gradstein et al., 2012), the duration from the FO of *Uniplanarius sissinghii* to the LO of *B. parca constricta* is proposed as 5.59 Myr. The uncertainty of the age of the two bioevents is calculated using a Compound Poisson Gamma law, applied to the problem of time-scale uncertainty (Haslett and Parnell, 2008; De Vleeschouwer and Parnell, 2014; Martinez and Dera, 2015, see supplementary information). The age uncertainty (2σ) of the FO of *U. sissinghii* is assessed as 0.54 Myr, and the age uncertainty (2σ) of the LO of *B. p. constricta* as 0.78 Myr. The duration from the FO of *U. sissinghii* to the LO of *B. p. constricta* with error margins is thus 5.59 ± 1.24 Myr (Table S3). In the Tercis-les-Bains section, the thickness between these two bioevents is 115.08 m, equivalent to an average sedimentation rate of 20.59 m/Myr, ranging from 16.65 to 26.95 m/Myr within the error margins. The 8.6-m wavelength, the highest-amplitude cycle in the $\delta^{13}C$ data (Fig. 5C), would thus correspond to an average period of 0.42 ± 0.1 Myr (Table S3), which is close to the period of the 405-kyr eccentricity (Laskar et al., 2004, 2011). The filtered signal on the band of 5–8 m allows the Tercis-les-Bains section to be divided into sequences of 405 kyr (Fig. 5B). The long-eccentricity cycle (405 kyr) identified at Tercis-les-Bains was also recognized using $CaCO_3$ data in the Lägerdorf–Kronsmoor section (northern Germany; Voigt and Schönfeld, 2010), from sediment gray level variations in the ODP Hole 762C (Exmouth Plateau; Thibault et al., 2012b) and in bulk carbonate $\delta^{13}C$ in the Bottaccione section (central Italy; Sprovieri et al., 2013).

Based on the 405-kyr sequences identified in the interval that spans the carbon–isotope negative shift (Figs. 5, 7), a total duration from the base of the pre-LCE to the top of the LCE is estimated as 1.3 Myr at Tercis-les-Bains. In the Lägerdorf–Kronsmoor record, the LCE as defined by Voigt et al. (2010) spans approximately two and a half 405-kyr cycles (UCa10, UCa9, and half of UCa8) and thus corresponds to a duration of *ca.* 1 Myr, while pre-LCE excursions span Uca7 and the upper half of UCa6 (Fig. 7). Here, we have attempted a correlation of 405-kyr eccentricity cycles identified from the $\delta^{13}C$ of Tercis-les-Bains to the 405-kyr eccentricity identified from the $CaCO_3$ of Lägerdorf–Kronsmoor (Fig. 7). This attempt is constrained by the correlation of carbon isotope events between the two sections, and in particular the *conica* Event, the pre-LCE excursions, the LCE and the CMBE (Fig. 7). From this correlation, it appears that several 405-kyr cycles are lacking at Tercis-les-Bains, supporting the inference that this section was affected by some short-term hiatuses, notably at the bottom and at the top of the LCE interval. However, the duration of the LCE appears rather similar at Tercis-les-Bains, spanning 800 to 900 kyr, while the pre-LCE spans another 400 kyr. Thus, the duration of the large perturbation of the carbon cycle affecting the Campanian, including both the pre-LCE and LCE, is estimated as *ca.* 1.3 Myr.

5.4. Relationship between clay mineralogy and $\delta^{13}C$

The clay mineral assemblages measured at Tercis-les-Bains and at Poigny are dominantly composed of smectite. This feature has been commonly observed in the Late Cretaceous clay sedimentation and attributed to hot semi-arid climatic conditions, high sea level, and volcanic activity (Chamley et al., 1990; Deconinck and Chamley, 1995; Jeans, 2006). Occasional detrital inputs are however prominent during the Campanian. A rise in detrital mineral content, including chlorite, illite, and kaolinite, is recorded in coincidence with the pre-LCE and LCE excursions (Fig. 3). At Poigny, the clay fraction of chalk shows an increase in detrital illite content at the expense of smectite from 111.5 to 61.5 m in depth (Deconinck et al., 2005; Fig. 4). Illite and chlorite are considered primary minerals originated from ancient rocks while kaolinite may be either reworked from the same detrital sources or from pedogenic blankets. As the three minerals fluctuate similarly, they probably have a common origin and their synchronous rise thus reflects increasing runoff. In that case, kaolinite cannot be taken as a good proxy of hydrolyzing conditions. This change in clay mineralogy starts within the pre-LCE interval and is fully expressed in the LCE interval. Perdiou et al. (2015) suggested that the pre-LCE interval corresponds to an amplification of the response of the carbon cycle to Milankovitch forcing prior to the LCE but did not discuss the main forcing environmental factors of these excursions. Here we show that, in both basins, the pre-LCE and LCE occurred during a period of increasing detrital inputs, which reflect enhanced erosion on continental massifs. Two hypotheses have been proposed to explain the illite input during the Late Campanian at Poigny: a climatic origin (cooling) or a tectonic episode (Riedel's Peine in the Paris Basin, Mortimore and Pomerol, 1997). More intensive erosion may also result from a sea-level fall. Eustatic variations indirectly affect the carbon cycle through changes in rates and sources of erosion. During the Campanian, sea-level changes have been correlated to $\delta^{13}C$ excursions (Jarvis et al., 2002, 2006). High sea level recorded during the Cretaceous led to the formation of many shelf seas and shallow environments. Such environments are associated with enhanced primary productivity (phytoplankton) and/or enhanced preservation of organic matter (OM) in anoxic environments. These conditions could have promoted OM burial, which may well explain the relationship between positive $\delta^{13}C$ excursions (SCBE and MCE) and transgressions (Jarvis et al., 2002, 2006). In contrast, negative $\delta^{13}C$ excursions during the Late Cretaceous have been associated to sea-level falls and, more specifically, the negative shift of the LCE has been associated with the *polyplocum* regression (Jarvis et al., 2002). Regression would have promoted erosion of the continents and the oxidation of OM by reworking continental and marine OM-rich levels (Jarvis et al., 2002, 2006; Voigt et al., 2012; Martinez and Dera, 2015), bringing isotopically light carbon to the oceans. It is therefore possible to propose a scenario for the LCE consistent with the observed isotopic and mineralogical data changes, considering that a drop in sea level was responsible for both a negative isotope excursion and a coeval detrital input. Further mineralogical and geochemical studies should be conducted on a wider scale to estimate the spatial extent of these changes.

5.5. Palaeotemperature trends

Bulk $\delta^{18}O$ values should be considered with caution, as the original signal can be easily altered by diagenesis. Calculations of temperature based on the equation of Anderson and Arthur (1983) using a $\delta^{18}O$ of seawater of −1‰ to account for the absence of a well-developed ice-sheet (Shackleton and Kennett, 1975) would yield values ranging from 27 °C at the base of the Campanian to 18 °C in the upper part of the Campanian at Poigny. These temperatures are lower than temperatures calculated by Linnert et al. (2014) from Tex_{86} data at the same latitude in subtropical marine environments, which probably indicates an offset of the bulk-rock $\delta^{18}O$ from original values during diagenesis. Nonetheless, temperature fluctuations can still be preserved in the trend of bulk-rock $\delta^{18}O$ if the studied series displays a homogeneous lithology (Jenkyns et al., 1994; Pellenard et al., 2014). As the Poigny borehole shows no major lithological change, the cooling trend potentially recorded here throughout the Campanian would be in agreement with the cooling of surface waters (Linnert et al., 2014) and bottom-waters (Friedrich et al., 2012) during this period.

5.6. Palaeoenvironmental scenario for the LCE

The additional Late Campanian isotopic and mineralogical data shown here offer new insights regarding the nature of the LCE. The increase in detrital flux in several sedimentary basins (Aquitaine Basin, Paris Basin, Umbria-Marches Basin, Saharan Platform) probably resulted from the intensification of continental erosion, and we estimate here a total duration of about 1.3 Myr for the large perturbation that comprises the LCE and pre-LCE. Geochemical data, notably the increase in the $^{87}Sr/^{86}Sr$ ratio recorded during the *R. calcarata* zone in the Postalm section (Wagreich et al., 2012), and during the LCE in the Lägerdorf–Kronsmoor section (McArthur et al., 1993), are also consistent with an intensification of continental weathering.

Higher levels of continental weathering can result from tectonic activity and/or sea-level changes. The Paris Basin experienced inversion processes during the Late Turonian (NE–SW compression), after an extensional period of subsidence (Albian to Turonian). The resulting deformation occurring during the Late Cretaceous (Guillocheau et al., 2000; Mansy et al., 2003) may have led to the observed stronger continental erosion. Otherwise, a global sea-level fall may have lowered base levels and enhanced erosion of continental areas as proposed by Jarvis et al. (2002, 2006) during the *polyplocum* event.

Continental erosion favored by newly exposed continental areas during the time interval spanned by the LCE would have ultimately led to consumption of atmospheric CO_2 through silicate weathering. The possible resulting decrease in the atmospheric pCO_2 could explain both the expression of the LCE and have contributed to the global cooling identified during the Campanian (Friedrich et al., 2012; Linnert et al., 2014).

This scenario can actually be tested through a simple isotope mass balance calculation. The postulated intensification of continental weathering lasted about 1.3 Myr, as estimated here from the duration of the interval from pre-LCE to LCE (*i.e.*, the interval of significant change in clay mineralogy). It is assumed here that the *ca.* 1.0‰ negative carbon isotope excursion recorded in the carbonate rocks was caused by a significant increase in continental weathering and by the oxidation of OM (Kump, 1991; Kump and Arthur, 1999; Jarvis et al., 2002, 2006). We have adapted here the simple model of Kump and Arthur (1999), with initial (pre-LCE) steady-state atmospheric pCO_2 estimated at 1200 ppmv (Hong and Lee, 2012), and isotopic composition of oceanic carbonates ($\delta^{13}C_{carb}$) estimated at +2.2‰. The more intense mid-ocean-ridge spreading of the Late Cretaceous leads us to increase the volcanic and metamorphic input of carbon by 30% (with regard to Phanerozoic average values proposed by Kump and Arthur, 1999). To reproduce the average 1.0‰ negative excursion of the LCE observed at Tercis-les-Bains and Poigny, the continental erosion needs to be multiplied by 1.5. As a consequence, total carbon burial would have increased by 50%.

In such a scenario, the increase in continental weathering significantly affects atmospheric pCO_2, which shows a rapid decrease from 1200 ppm to ~660 ppm. This drop in the atmospheric pCO_2 may have induced a cooling after the LCE, which is consistent with the isotopic data from the El Kef section (Tunisia; Jarvis et al., supplementary material, 2002) and from the Shuqualak–Evans borehole (Mississipi, USA, Linnert et al., 2014). This mechanism may explain the cooling phase observed in the Late Campanian–Maastrichtian (Friedrich et al., 2012; Linnert et al., 2014).

6. Conclusions

The integrated use of data from clay mineralogy and stable isotope geochemistry (^{18}O, ^{13}C) reveals that a significant increase in detrital inputs of illite and/or chlorite and kaolinite occurred in the Paris and Aquitaine basins during the time interval spanning the $\delta^{13}C$ pre-LCE and LCE. This finding argues for the intensification of the hydrological cycle and/or of continental erosion at that time.

Based on cyclostratigraphic analyses performed on the $\delta^{13}C$ of the Tercis-les-Bains section, the duration of the interval from the start of pre-LCE to LCE is estimated as *ca.* 1.3 Myr at least. The duration of LCE *sensu stricto* is estimated here as 0.8–0.9 Myr.

The more intense weathering of continental areas during the LCE was favored by a vast exposure of continents *via* the post-Turonian tectonic activity and enhanced by the *polyplocum* regression. Intense weathering is probably responsible for a pCO_2 decrease, which would have contributed to a global cooling in the Late Campanian.

Acknowledgments

We thank Tercis-les-Bains town council for providing access to the quarry and Dr. C. Robin (University of Rennes) for providing access to the Poigny borehole. The constructive reviews by two anonymous reviewers and by the editor, Pr. T.J. Algeo, have greatly contributed to the study. We also thank them and Dr. C. Chateau-Smith for helpful suggestions about English usage. This work forms part of the Anox-Sea and ASTS-CM (Astronomical Time Scale for the Cenozoic and Mesozoic Era) projects, both of which are funded by the French National Agency for Research (ANR).

Appendix A. Supplementary data

Supplementary data to this article can be found online at http://dx.doi.org/10.1016/j.palaeo.2016.01.040.

References

Algeo, T.J., Meyers, P.A., Robinson, R.S., Rowe, H., Jiang, G.Q., 2014. Icehouse–greenhouse variations in marine denitrification. Biogeosciences 11 (4), 1273–1295.

Anderson, T.F., Arthur, M.A., 1983. Stable isotopes of oxygen and carbon and their application to sedimentologic and paleoenvironmental problems. In: Arthur, M.A., Anderson, T.F., Kaplan, I.R., Veizer, J., Land, L.S. (Eds.), Stable Isotopes in Sedimentary Geology. SEPM Short Course, 10. Tulsa, pp. 1–151.

Auclair, A.-C., Joachimski, M.M., Lécuyer, C., 2003. Deciphering kinetic, metabolic and environmental controls on stable isotope fractionations between seawater and the shell of *Terebratalia transversa* (brachiopoda). Chem. Geol. 202, 59–78.

Barrera, E., 1994. Global environmental changes preceding the Cretaceous–Tertiary boundary: early–late Maastrichtian transition. Geology 22, 877–880.

Barrera, E., Savin, S.M., 1999. Evolution of Campanian–Maastrichtian marine climates and oceans. Geol. Soc. Am. Spec. Pap. 332, 245–282.

Barrera, E., Savin, S.M., Thomas, E., Jones, C.E., 1997. Evidence for thermohaline-circulation reversals controlled by sea-level change in the latest Cretaceous. Geology 25, 715–718.

Berthou, P.Y., Odin, G.S., Antonescu, E., Villain, J.M., 2001. Chapitre B1b. Microfaciès des sédiments du Campanien et du Maastrichtien de Tercis-les-Bains (Landes, France). In: Odin, G.S. (Ed.), The Campanian–Maastrichtian Stage Boundary Characterisation at Tercis-les-Bains (France) and Correlation with Europe and Other Continents. Developments in Palaeontology and Stratigraphy. Elsevier, Amsterdam, pp. 113–119.

Bilotte, M., Odin, G.S., Vrielynck, B., 2001. Chapter A4 geology and late cretaceous palaeogeography of the geological site at Tercis-les-Bains (Landes, France). In: Odin, G.S. (Ed.), The Campanian–Maastrichtian Stage Boundary Characterisation at Tercis-les-Bains (France) and Correlation with Europe and Other Continents. Developments in Palaeontology and Stratigraphy. Elsevier, Amsterdam, pp. 47–59.

Blakey, R.C., 2008. Gondwana paleogeography from assembly to breakup—a 500 m.y. odyssey. In: Fielding, C.R., Frank, T.D., Isbell, J.L. (Eds.), Resolving the Late Paleozoic Ice Age in Time and Space. Geological Society of America Special Paper 441, pp. 1–28.

Brunet, M.-F., Le Pichon, X., 1982. Subsidence of the Paris Basin. J. Geophys. Res. 87 (10), 8547–8560.

Chamley, H., Maillot, H., Duée, G., Robert, C., 1984. Paleoenvironmental history of the Walvis Ridge at the Cretaceous–Tertiary transition, from mineralogical and geochemical investigations. Initial Rep. Deep Sea Drill. Proj. 74, 685–695.

Chamley, H., Deconinck, J.-F., Millot, G., 1990. Sur l'abondance des minéraux smectitiques dans les sédiments marins communs déposés lors des périodes de haut niveau marin du Jurassique supérieur au Paléogène. Compte Rendu de l'Académie des Sciences de Paris, Tome 311, Série II, pp. 1529–1536.

Clarke, L.J., Jenkyns, H.C., 1999. New oxygen isotope evidence for long-term Cretaceous climatic change in the Southern Hemisphere. Geology 27, 699–702.

Deconinck, J.-F., 1992. Sédimentologie des argiles dans le Jurassique-Crétacé d'Europe occidentale et du Maroc. Mémoire d'Habilitation à Diriger des Recherches (HDR). Université de, Lille 248 pages.

Deconinck, J.-F., Chamley, H., 1995. Diversity of smectite origins in Late Cretaceous sediments: example of chalks from northern France. Clay Miner. 30 (4), 365–380.

Deconinck, J.-F., Amédro, F., Baudin, F., Godet, A., Pellenard, P., Robaszynski, F., Zimmerlin, I., 2005. Late Cretaceous palaeoenvironments expressed by the clay mineralogy of Cenomanian–Campanian chalks from the east of the Paris Basin. Cretac. Res. 26, 171–179.

De Vleeschouwer, D., Parnell, A.C., 2014. Reducing time-scale uncertainty for the Devonian by integrating astrochronology and Bayesian statistics. Geology 42 (6), 491–494.

Dewey, J.F., Pitman, W.C., Ryan, W.B.F., Bonnin, J., 1973. Plate tectonics and the evolution of the Alpine system. Geol. Soc. Am. Bull. 84 (10), 3137–3180.

Friedrich, O., Herrle, P.A., Wilson, M.J., Cooper, J., Erbacher, J., Hemleben, C., 2009. Early Maastrichtian carbon cycle perturbation and cooling event: implications from the South Atlantic Ocean. Paleoceanography 24 (2), 1–14.

Friedrich, O., Norris, R.D., Erbacher, J., 2012. Evolution of Middle to Late Cretaceous oceans—a 55 m.y. record of Earth's temperature and carbon cycle. Geology 40, 107–110.

Gardin, S., Odin, G.S., Bonnemaison, M., Melinte, M., Monechi, S., von Salis, K., 2001. Chapter C3e results of the cooperative study on the calcareous nannofossils across the Campanian–Maastrichtian boundary at Tercis-les-Bains (Landes, France). In: Odin, G.S. (Ed.), The Campanian–Maastrichtian Stage Boundary Characterisation at Tercis-les-Bains (France) and Correlation with Europe and Other Continents. Developments in Palaeontology and Stratigraphy. Elsevier, Amsterdam, pp. 293–309.

Gardin, S., Galbrun, B., Thibault, N., Coccioni, R., Silva, I.P., 2012. Bio-magnetochronology for the upper Campanian–Maastrichtian from the Gubbio area, Italy: new results from the Contessa Highway and Bottaccione sections. Newsl. Stratigr. 45, 75–103.

Gillikin, D.P., Lorrain, A., Bouillon, S., Willenz, P., Dehairs, F., 2006. Stable carbon isotopic composition of *Mytilus edulis* shells: relation to metabolism, salinity, salinity, $\delta^{13}C_{DIC}$ and phytoplankton. Org. Geochem. 37, 1371–1382.

Gradstein, F.M., Ogg, J.G., Schmitz, M.D., Ogg, G.M., 2012. The Geologic Time Scale 2012. 2. Elsevier BV, Amsterdam, The Netherlands 1176 pages.

Guillocheau, F., Robin, C., Allemand, P., Bourquin, S., Brault, N., Dromart, G., Friedenberg, R., Garcia, J.-P., Gaulier, J.-M., Gaumet, F., Grosdoy, B., Hanot, F., Le Strat, P., Mettraux, M., Nalpas, T., Prijac, C., Rigollet, C., Serrano, O., Grandjean, G., 2000. Meso-Cenozoic geodynamic evolution of the Paris Basin: 3D stratigraphic constraints. Geodynamica Acta 13, 189–245.

Haq, B.U., Hardenbol, J., Vail, P.R., 1987. Chronology of fluctuating sea levels since the Triassic. Science 235, 1156–1167.

Haslett, J., Parnell, A., 2008. A simple monotone process with application to radiocarbon-dated depth chronologies. Appl. Stat. 57 (4), 399–418.

Hong, S.K., Lee, Y.I., 2012. Evaluation of atmospheric carbon dioxide concentrations during the Cretaceous. Earth Planet. Sci. Lett. 327-328, 23–28.

Huber, B.T., Hodell, D.A., Hamilton, C.P., 1995. Middle–Late Cretaceous climate of the southern high latitudes: stable isotopic evidence for minimal equator-to-pole thermal gradients. Geol. Soc. Am. Bull. 107, 1164–1191.

Inoue, A., Bouchet, A., Velde, B., Meunier, A., 1989. Convenient technique for estimating smectite layer percentage in randomly interstratified illite/smectite minerals. Clay Clay Miner. 37 (3), 227–234.

Jarvis, I., Mabrouk, A., Moody, R.T., de Cabrera, S., 2002. Late Cretaceous (Campanian) carbon isotope events, sea-level change and correlation of the Tethyan and Boreal realms. Palaeogeogr. Palaeoclimatol. Palaeoecol. 188, 215–248.

Jarvis, I., Gale, A.S., Jenkyns, H.C., Pearce, M.A., 2006. Secular variation in late cretaceous carbon isotopes: a new $\delta^{13}C$ carbonate reference curve for the Cenomanian–Campanian (99.6–70.6 Ma). Geol. Mag. 143, 561–608.

Jeans, C.V., 2006. Clay mineralogy of the cretaceous strata of the British Isles. Clay Miner. 41, 47–150.

Jenkyns, H.C., Gale, A.S., Corfield, R.M., 1994. Carbon- and oxygen-isotope stratigraphy of the English Chalk and Italian Scaglia and its palaeoclimatic significance. Geol. Mag. 131, 1–34.

Jung, C., Voigt, S., Friedrich, O., 2012. High-resolution carbon–isotope stratigraphy across the Campanian–Maastrichtian boundary at Shatsky Rise (tropical Pacific). Cretac. Res. 37, 177–185.

Kirby, M.X., Soniat, T.M., Spero, H.J., 1998. Stable isotope sclerochronology of Pleistocene and recent oyster shells (*Crassostrea virginica*). PALAIOS 13, 560–569.

Kump, L.R., 1991. Interpreting carbon–isotope excursions: strangelove oceans. Geology 19, 299–302.

Kump, L.R., Arthur, M.A., 1999. Interpreting carbon–isotope excursions: carbonates and organic matter. Chem. Geol. 161, 181–198.

Laskar, J., Robutel, P., Joutel, F., Gastineau, M., Correia, A.C.M., Levrard, B., 2004. A long-term numerical solution for the insolation quantities of the Earth. Astron. Astrophys. 428, 261–285.

Laskar, J., Fienga, A., Gastineau, M., Manche, H., 2011. La2010: a new orbital solution for the long-term motion of the Earth. Astron. Astrophys. 532, 1–17.

Lasseur, E., 2007. La Craie du Bassin de Paris (Cénomanien-Campanien, Crétacé supérieur). Sédimentologie de faciès, stratigraphie séquentielle et géométrie 3D. Unpublished PhD Université Rennes 1, 409 pages.

Le Callonnec, L., Renard, M., Pomerol, B., Janodet, C., Caspard, E., 2000. Données géochimiques préliminaires sur la série Cénomano-campanienne des forages 701 et 702 du programme Craie 700. Bull. Inf. Géol. Bassin Paris 37 (2), 112–119.

Lewy, Z., Odin, G.S., 2001. Chapter B2d magnetostratigraphy across the Campanian–Maastrichtian boundary at Tercis-les-Bains in comparison with northern Germany, the Apennines (Central Italy) and North America; biostratigraphical and geochronological constraints. In: Odin, G.S. (Ed.), The Campanian–Maastrichtian Stage Boundary Characterisation at Tercis-les-Bains (France) and Correlation with Europe and Other Continents. Developments in Palaeontology and Stratigraphy. Elsevier, Amsterdam, pp. 175–183.

Li, L., Keller, G., Adatte, T., Stinnesbeck, W., 2000. Late Cretaceous sea-level changes in Tunisia: a multi-disciplinary approach. J. Geol. Soc. 157, 447–458.

Linnert, C., Robinson, S.A., Lees, J.A., Bown, P.R., Pérez-Rodríguez, I., Petrizzo, M.R., Falzoni, F., Littler, K., Arz, J.A., Russell, E.E., 2014. Evidence for global cooling in the Late Cretaceous. Commun. 5, 1–7.

Mansy, J.-L., Manby, G.M., Averbuch, O., Everaerts, M., Bergerat, F., Van Vliet-Lanoe, B., Lamarche, J., Vandycke, S., 2003. Dynamics and inversion of the Mesozoic Basin of the Weald–Boulonnais area: role of basement reactivation. Tectonophysics 373 (1), 161–179.

Martinez, M., Deconinck, J.-F., Pellenard, P., Reboulet, S., Riquier, L., 2013. Astrochronology of the Valanginian Stage from reference sections (Vocontian Basin, France) and palaeoenvironmental implications for the Weissert Event. Palaeogeogr. Palaeoclimatol. Palaeoecol. 376, 91–102.

Martinez, M., Deconinck, J.-F., Pellenard, P., Riquier, L., Company, M., Reboulet, S., 2015. Astrochronology of the Valanginian-Hauterivian stages (Early Cretaceous): chronological relationships between the Paraná–Etendeka large igneous province, the Weissert and the Faraoni events. Glob. Planet. Chang. 131, 158–173.

Martinez, M., Dera, G., 2015. Orbital pacing of carbon fluxes by a ~9-My eccentricity cycle during the Mesozoic. Proc. Natl. Acad. Sci. 112 (41), 12604–12609. http://dx.doi.org/10.1073/pnas.1419946112.

McArthur, J.M., Thirlwall, M.F., Chen, M., Gale, A.S., Kennedy, W.J., 1993. Strontium isotope stratigraphy in the Late Cretaceous: numerical calibration of the Sr isotope curve and intercontinental correlation for the Campanian. Paleoceanography 8 (6), 859–873.

McConnaughey, T.A., 1989a. ^{13}C and ^{18}O disequilibrium in biological carbonates: I. Patterns Geochim. Cosmochim. Acta 53, 151–162.

McConnaughey, T.A., 1989b. ^{13}C and ^{18}O disequilibrium in biological carbonates: II. In vitro simulation of kinetic isotope effects. Geochim. Cosmochim. Acta 53, 163–171.

McConnaughey, T.A., Burdett, J., Whelan, J.F., Paul, C.K., 1997. Carbon isotopes in biological carbonates: respiration and photosynthesis. Geochim. Cosmochim. Acta 61, 611–622.

Mégnien, C., Hanot, F., 2000. Programme craie 700: Deux forages scientifiques profonds pour étudier les phénomènes diagénétiques de grande ampleur dans la craie du Bassin de Paris. Bull. Inf. Géol. Bassin Paris 37 (2), 3–7.

Melinte, M., Odin, G.S., 2001. Chapter C3d Optical study of the calcareous nannofossils from Tercis-les-Bains (Landes, France) across the Campanian–Maastrichtian boundary. In: Odin, G.S. (Ed.), The Campanian–Maastrichtian Stage Boundary Characterisation at Tercis-les-Bains (France) and Correlation with Europe and Other Continents. Developments in Palaeontology and Stratigraphy. Elsevier, Amsterdam, pp. 285–292.

Meyers, S.R., 2012. Seeing red in cyclic stratigraphy: spectral noise estimation for astrochronology. Paleoceanography 27, PA3228.

Meyers, S.R., 2014. astrochron: An R Package for Astrochronology. http://cran.r-project.org/package=astrochron.

Mettraux, M., Homewood, P., Schwab, A., Guillocheau, F., 1999. Sedimentology and accommodation cycles of Paris Basin Campanian Chalk: the key to high-resolution stratigraphy and seismic signature. Special Publications of SEPM, pp. 317–334.

Moore, D.M., Reynolds, R.C., 1997. X-Ray Diffraction and the Identification and Analysis of Clay Minerals. second ed. Oxford University Press, Oxford; New York (378 pages).

Mortimore, R., Pomerol, B., 1997. Upper Cretaceous tectonic phases and end Cretaceous inversion in the Chalk of the Anglo-Paris Basin. Proc. Geol. Assoc. 108, 231–255.

Odin, G.S., 2001. Chapter B1a Descriptive lithostratigraphy of the Campanian–Maastrichtian succession at Tercis-les-Bains (SW France). In: Odin, G.S. (Ed.), Developments in Palaeontology and Stratigraphy, the Campanian–Maastrichtian Stage Boundary Characterisation at Tercis-les-Bains (France) and Correlation with Europe and Other Continents. Elsevier, Amsterdam, pp. 85–112.

Odin, G.S., Amorosi, A., 2001. Chapter B1c interpretative reading of the Campanian–Maastrichtian deposits at Tercis-les-Bains: sedimentary breaks, rhythms, accumulation rate, sequences. In: Odin, G.S. (Ed.), The Campanian–Maastrichtian Stage Boundary Characterisation at Tercis-les-Bains (France) and Correlation with Europe and Other Continents. Developments in Palaeontology and Stratigraphy. Elsevier, Amsterdam, pp. 120–133.

Odin, G.S., Lamaurelle, M.A., 2001. The global Campanian–Maastrichtian stage boundary. Episodes 24, 229–238.

Odin, G.S., Arz, J.A., Caron, M., Ion, J., Molina, E., 2001a. Chapter C5d Campanian–Maastrichtian planktonic foraminifera at Tercis-les-Bains (Landes, France); synthetic view and potential for global correlation. In: Odin, G.S. (Ed.), The Campanian–Maastrichtian Stage Boundary Characterisation at Tercis-les-Bains (France) and

Correlation with Europe and Other Continents. Developments in Palaeontology and Stratigraphy. Elsevier, Amsterdam, pp. 379–395.
Odin, G.S., Courville, P., Machalski, M., Cobban, W.A., 2001b. Chapter D4g the Campanian–Maastrichtian ammonite fauna from Tercis-les-Bains (Landes, France); a synthetic view. In: Odin, G.S. (Ed.), The Campanian–Maastrichtian Stage Boundary Characterisation at Tercis-les-Bains (France) and Correlation with Europe and Other Continents. Developments in Palaeontology and Stratigraphy. Elsevier, Amsterdam, pp. 550–567.
Pellenard, P., Deconinck, J.-F., 2006. Mineralogical variability of Callovo–Oxfordian clays from the Paris Basin and the Subalpine Basin. Compt. Rendus Geosci. 338 (12), 854–866.
Pellenard, P., Tramoy, R., Pucéat, E., Huret, E., Martinez, M., Bruneau, L., Thierry, J., 2014. Carbon cycle and sea-water palaeotemperature evolution at the Middle–Late Jurassic transition, eastern Paris Basin (France). Mar. Pet. Geol. 53, 30–43.
Perdiou, A., Thibault, N., Anderskouv, K., van Buchem, F., Buijs, G.J.A., Bjerrum, C.J., 2015. Orbital calibration of the late Campanian carbon isotope event in the North Sea. J. Geol. Soc. Lond. http://dx.doi.org/10.1144/jgs2015-120 (in press).
Petschick, R., 2000. MacDiff Ver. 4.2.3. Manual Geologisch-Palaontologisches Institute Johann Wolfgang Goethe Universitat Frankfurt Main senckenberganlage. pp. 32–34.
Philip, J., Floquet, M., 2000. Early Campanian (83–80.5 Ma) Coord. In: Crasquin, S. (Ed.), Atlas Peri-Tethys, Palaeogeographic maps. Explanatory notes. Commission for the Geological Map of the World (CCGM/CCMW), Paris, pp. 145–152.
Pucéat, E., Lécuyer, C., Reisberg, L., 2005. Neodymium isotope evolution of NW Tethyan Upper Ocean waters throughout the Cretaceous. Earth Planet. Sci. Lett. 236, 705–720.
Robaszynski, F., Gonzáles Donoso, J.M., Linares, D., Amédro, F., Caron, M., Dupuis, C., Dhondt, A.V., Gartner, S., 2000. Le Crétacé Supérieur de la région de Kalaat Senan, Tunisie centrale. Litho- Biostratigraphie intégrée: Zone d'ammonites, de foraminifères planctoniques et de nannofossiles du Turonien Supérieur au Maastrichtien. Bulletin des Centres de Recherches Elf-Aquitaine Exploration-Production 22 (2), pp. 35–490.
Robaszynski, F., Pomerol, B., Masure, E., Bellier, J.-P., Deconinck, J.-F., 2005. Stratigraphy and stage boundaries in reference sections of the Upper Cretaceous Chalk in the east of the Paris Basin: the "Craie 700" Provins boreholes. Cretac. Res. 26, 157–169.
Scholle, P.A., Arthur, M.A., 1980. Carbon isotope fluctuations in Cretaceous pelagic limestones: potential stratigraphic and petroleum exploration tool. AAPG Bull. 64 (1), 67–87.
Shackleton, N.J., Kennett, J.P., 1975. Late Cenozoic oxygen and carbon isotopic changes at DSDP Site 284: implications for glacial history of the Northern Hemisphere and Antarctica. Initial Reports of the Deep Sea Drilling Project, 29:801–7. US Government Printing Office, Washington, DC, pp. 801–807.
Smith, A.G., 1971. Alpine deformation and the oceanic areas of the Tethys, Mediterranean, and Atlantic. Geol. Soc. Am. Bull. 82 (8), 2039–2070.
Środoń, J., 2009. Quantification of illite and smectite and their layer charges in sandstones and shales from shallow burial depth. Clay Miner. 44, 421–434. http://dx.doi.org/10.1180/claymin.2009.044.4.421.
Sprovieri, M., Sabatino, N., Pelosi, N., Batenburg, S.J., Coccioni, R., Iavarone, M., Mazzola, S., 2013. Late cretaceous orbitally-paced carbon isotope stratigraphy from the Bottaccione Gorge (Italy). Palaeogeogr. Palaeoclimatol. Palaeoecol. 379–380, 81–94. http://dx.doi.org/10.1016/j.palaeo.2013.04.006.
Taner, M.T., 2003. Attributes Revisited. Technical Publication, Rock Solid Images, Inc., Houston, Texas. URL: http://www.rocksolidimages.com/pdf/attrib_revisited.htm.
Thibault, N., Harlou, R., Schovsbo, N., Schiøler, P., Minoletti, F., Galbrun, B., Lauridsen, B.W., Sheldon, E., Stemmerik, L., Surlyk, F., 2012a. Upper Campanian–Maastrichtian nannofossil biostratigraphy and high-resolution carbon–isotope stratigraphy of the Danish Basin: towards a standard $\delta^{13}C$ curve for the Boreal Realm. Cretac. Res. 33, 72–90.
Thibault, N., Husson, D., Harlou, R., Gardin, S., Galbrun, B., Huret, E., Minoletti, F., 2012b. Astronomical calibration of upper Campanian–Maastrichtian carbon isotope events and calcareous plankton biostratigraphy in the Indian Ocean (ODP Hole 762C): implication for the age of the Campanian–Maastrichtian boundary. Palaeogeogr. Palaeoclimatol. Palaeoecol. 337-338, 52–71.
Thibault, N., Jelby, M.E., Anderskouv, K., Bjerager, M., Surlyk, F., 2015. Upper Campanian–Maastrichtian chronostratigraphy of the Skælskør-1 core (eastern Sjælland, Danish Basin): correlation at the basin and global scale and paleoclimatic changes. Lethaia http://dx.doi.org/10.1111/let.12128.
Thomson, D.J., 1982. Spectrum estimation and harmonic-analysis. Proceedings of the Institute of Electrical and Electronics Engineers (IEEE) 70, pp. 1055–1096.
Thomson, D.J., 1990. Quadratic-inverse spectrum estimates—applications to paleoclimatology. Philosophical Transactions: Physical Sciences and Engineering, the Royal Society 332, pp. 539–597.
Voigt, S., Friedrich, O., Norris, R., Schönfeld, J., 2010. Campanian–Maastrichtian carbon isotope stratigraphy: shelf-ocean correlation between the European shelf sea and the tropical Pacific Ocean. Newsl. Stratigr. 44, 57–72.
Voigt, S., Schönfeld, J., 2010. Cyclostratigraphy of the reference section for the Cretaceous white chalk of northern Germany, Lägerdorf–Kronsmoor: a Late Campanian–Early Maastrichtian orbital time scale. Palaeogeogr. Palaeoclimatol. Palaeoecol. 287, 67–80.
Voigt, S., Gale, A.S., Jung, C., Jenkyns, H.C., 2012. Global correlation of upper Campanian–Maastrichtian successions using carbon–isotope stratigraphy: development of a new Maastrichtian timescale. Newsl. Stratigr. 45, 25–53.
Wagreich, M., Hohenegger, J., Neuhuber, S., 2012. Nannofossil biostratigraphy, strontium and carbon isotope stratigraphy, cyclostratigraphy and an astronomically calibrated duration of the Late Campanian *Radotruncana calcarata* zone. Cretac. Res. 38, 80–96.
Walaszczyk, I., Cobban, W.A., Odin, G.S., 2002. The inoceramid succession across the Campanian–Maastrichtian boundary. Bull. Geol. Soc. Den. 49, 53–60.
Wendler, I., 2013. A critical evaluation of carbon isotope stratigraphy and biostratigraphic implications for late cretaceous global correlation. Earth Sci. Rev. 126, 116–146. http://dx.doi.org/10.1016/j.earscirev.2013.08.003.
Wenzel, B., Lécuyer, C., Joachimski, M., 2000. Comparing oxygen isotope records of Silurian calcite and phosphate—$\delta^{18}O$ compositions of brachiopods and conodonts. Geochimi. Cosmochimi. Acta 64 (11), 1859–1872.